Supplementary Information (SI) for Materials Advances.

Modification of ZnO gas-diffusion-electrodes for enhanced electrochemical CO_2 reduction: Optimization of operational conditions and mechanism investigation.

Gonçalves J. Marrenjo,[1,2] Gelson T. S. T. da Silva,[3] Rodrigo A. Muñoz,[1] Lucia H. Mascaro,[3] Osmando F. Lopes[1,*]

[1] *Institute of Chemistry, Federal University of Uberlândia, Avenida João Naves de Avila, 2121, 34800-902 Uberlândia, Minas Gerais, Brazil*

[2] *Save University, Department of Natural Sciences, FPLM Avenida FPLM, 111, +25829371110, Massinga, Inhambane, Mozambique.*

[3.] *Interdisciplinary Laboratory of Electrochemistry and Ceramics, Department of Chemistry, Federal University of Sao Carlos, São Carlos, São Paulo, 13565-905, Brazil*

EXPERIMENTAL SECTION

Characterization

The thermogravimetric analysis (TGA) was performed using a TA Instruments Shimadzu DTG-60H thermogravimetric analyzer in a temperature range of 20 to 600°C under a synthetic air flow, applying a heating rate of 10°C/minute. The crystallinity of the samples was analyzed by X-ray diffraction (XRD) using Cu Kα radiation (λ=1.5406Å) in the 2θ range of 10 to 70° with a Shimadzu XRD-6000 diffractometer. Raman spectra were obtained using a Confocal Raman spectrometer, LabRAM HR Evolution model – HORIBA, with a CCD Sensor (OSD Syncerity) customized with 4 laser lines, coupled with HORIBA Scientific's LabSpec software. A 532nm excitation wavelength was applied, generating a power of 50mW, measured with a power meter as 78mW. Infrared spectra (FTIR) of the materials were acquired using a Perkin Elmer FTIR Frontier Single Range – MIR spectrophotometer in the range of 4000 to 220 cm^{-1} with 9 scans and a resolution of 4 cm^{-1}. Measurements were performed using an Attenuated Total Reflectance (ATR) accessory with a diamond crystal. The morphologies of the samples were examined by scanning electron microscopy (SEM) using a Tescan VEGA 3 LMU microscope equipped with a thermionic emission electron source, coupled with a microanalysis detector for elemental identification.

The calculation of crystal size was performed using the Scherrer Equation. (S1).

$$Dhkl=\frac{KY}{\beta COS(\theta)} \quad \text{Eq. (S1).}$$

Where D is the crystal size, Cu Kα (1.54 Å) is the wavelength of the radiation, β is the full width at half maximum (FWHM) in radians, k is the shape factor (0.9), and θ is the scattering angle.

The faradaic efficiencies of CO and H_2 were calculated using Equation (S2)

$$FE = \frac{(2nF \times 100\%)}{Q} \qquad \text{Eq.(S2)}$$

2 is relates with the number of electrons involved in the electrochemical reduction of CO_2 to CO or H_2, **n**-is the number of moles of products, **F**-is 96.485 $C \cdot mol^{-1}$ (Faraday's constant), and **Q**-is the total transferred charge.

Table S1. The crystallite size of ZnO treated at different temperatures and modified with monoethanolamine was determined using the Scherrer equation.

Samples	Xc	Wc	D (nm)	Crystalline phase
ZnO-100	36.27758	0.20039	41.722	ZnO
ZnO-150	36.27712	0.20015	41.772	ZnO
ZnO/Met-31 µL	36.27769	0.20037	41.726	ZnO

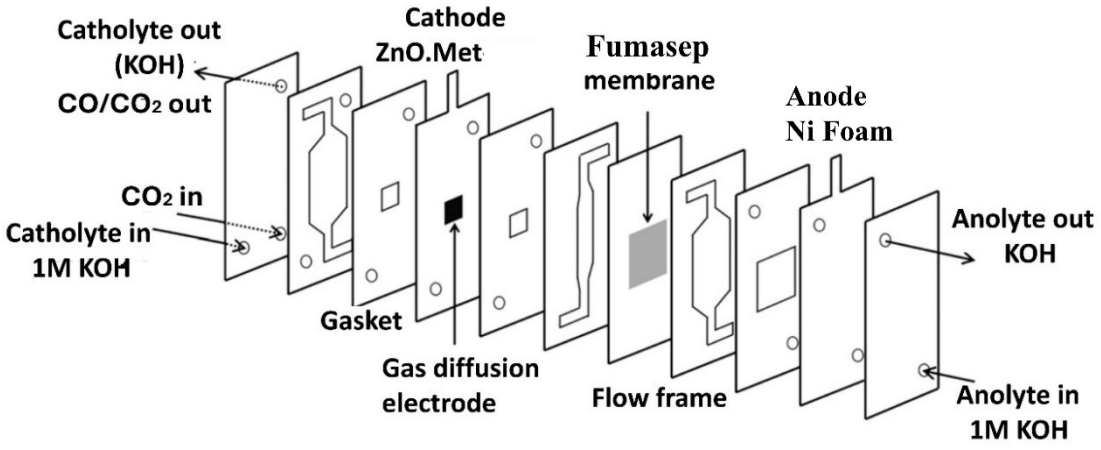

Figure S1. Configuration of the commercial flow cell (Micro Flow Cell, Electrocell) with three compartments.

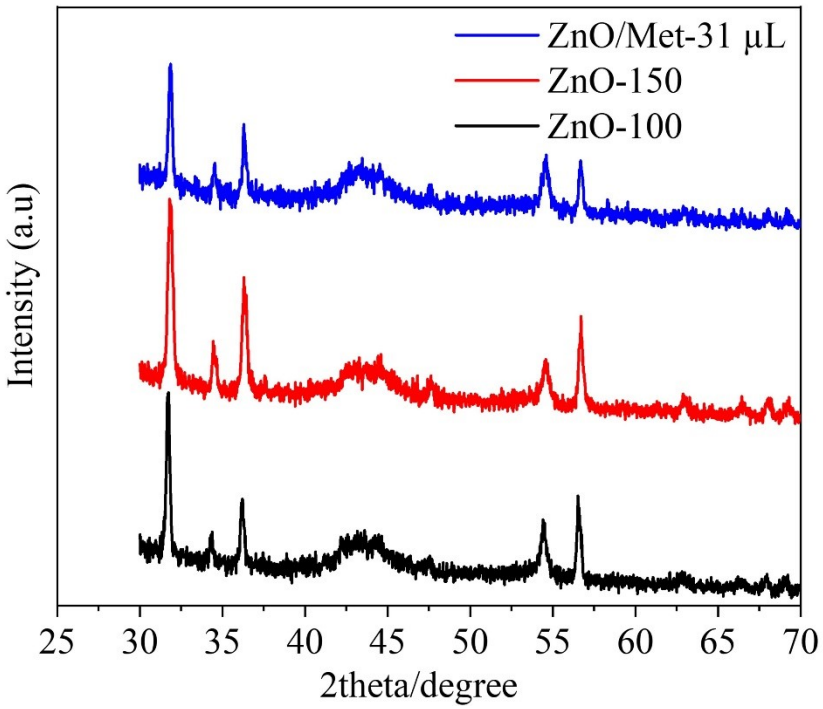

Figure. S2*:* X-ray diffraction (XRD) patterns of ZnO electrodes prepared at different temperatures (100 and 150 °C) and modified with monoethanolamine (ZnO/Met-31 µL).

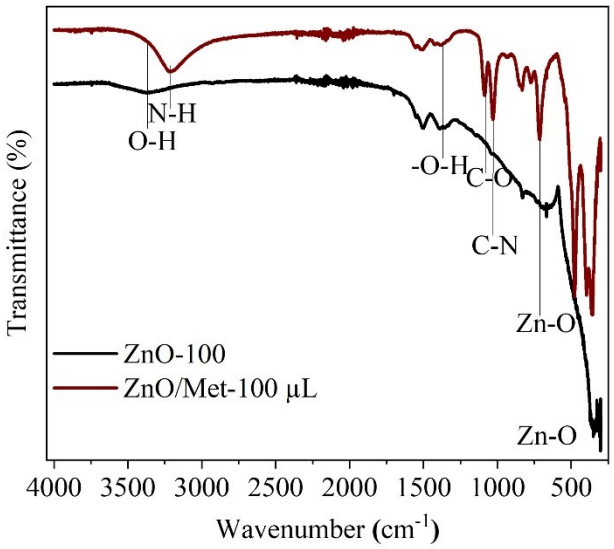

Figure S3: FTIR spectra of ZnO-100 and ZnO/Met-100 µL.

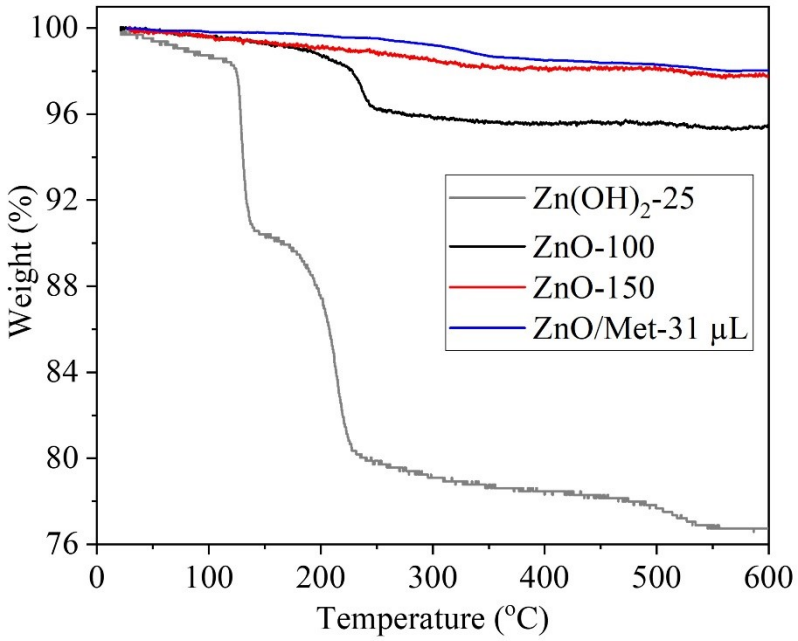

Figure. S4: A) Thermogravimetric analysis of the precursor $Zn(OH)_2$ and ZnO obtained by hydrothermal treatment at 100°C, 150°C, and ZnO/Met-31µL .

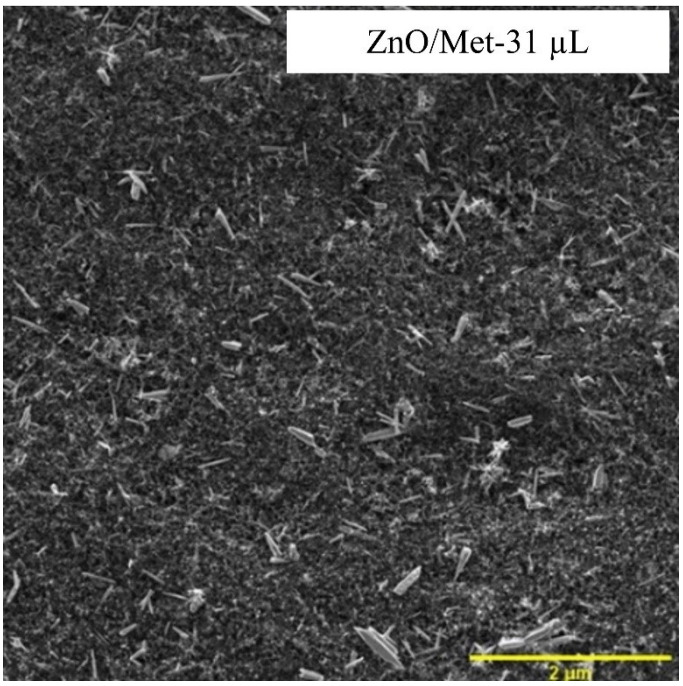

Figure S5. SEM image of the surface of the ZnO/Met-31 µL electrode with 25% CB.

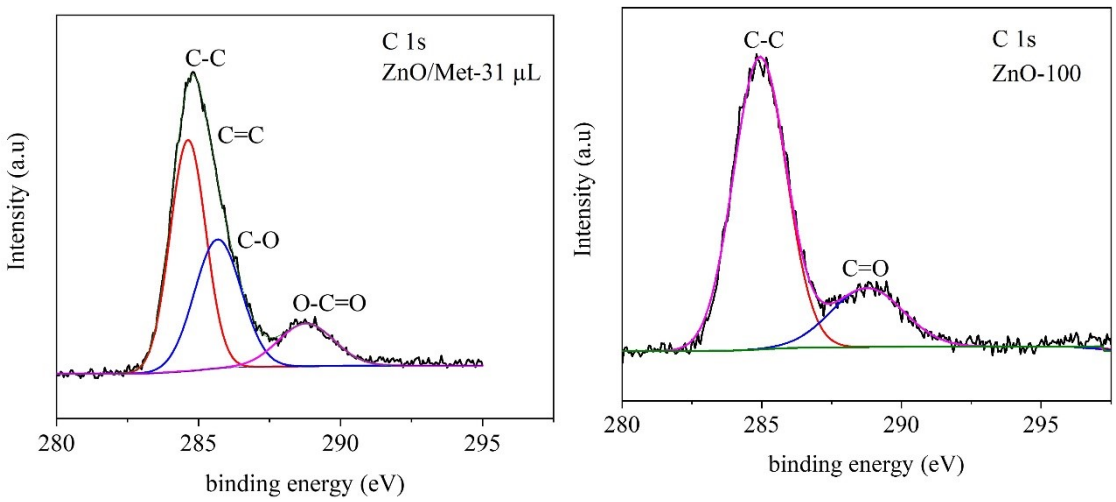

Figure S6. High resolution spectra of carbon C1s used to calibrate the binding energies for A) ZnO/Met-31 µL and B) ZnO-100 samples.

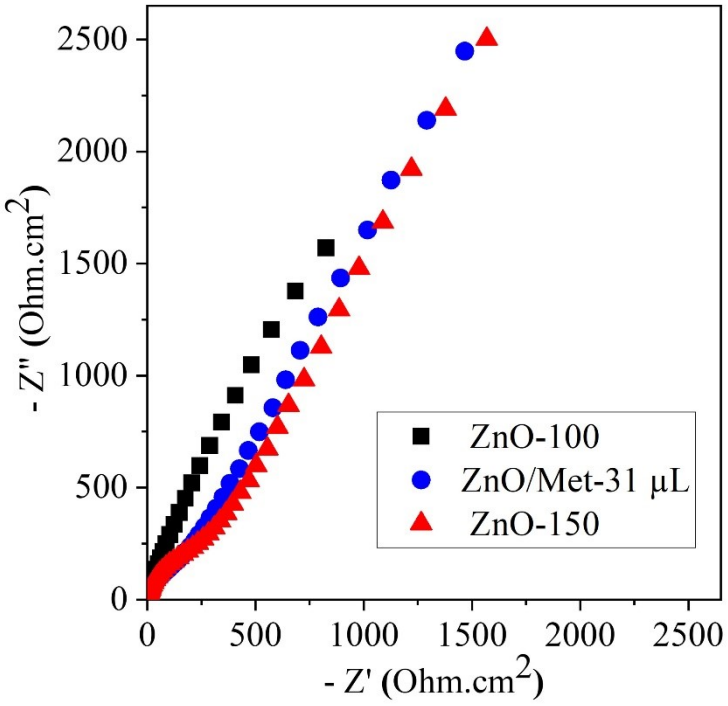

Figure S7. Nyquist plot of the impedance (EIS) of GDEs loaded with the catalysts studied under ECR conditions at open circuit potential.

Table S2: Comparison of this work with other materials and systems studied for CO production.

Catalyst	System	FE CO (%)	j (mA.cm^{-2})	E (V)	Stability	Electrolyte	Ref.
ZnO	Flow cell	> 80	-130	-1.2 V vs RHE	100 h	1 M KOH	**
ZnO	MEA	82	-200	−1.2 V vs RHE	>100 h	1 M KOH	[1]
Zn- foam	Flow cell	85	-200	-0.64 V vs RHE	>10 h	1 M KOH	[2]
Zn	MEA	> 90	-200	-3 V	-	1 M KOH	[3]
Oxide-derived Zn	Flow cell	90	-200	-0.62 V vs Ag/AgCl	>18 h	0.1 M $KHCO_3$	[4]
OD-Zn	Flow cell	80	-100	-0.6 V Ag/AgCl	>10 h	2.0 M $KHCO_3$	[5]
ZnO	Flow cell	90	140	-0.8 V vs RHE	-	1 M KOH	[6]
ZnS/ZnO	Flow cell	92	327	-0.7 V vs RHE	40 h	1 M KOH	[7]

** This work

References

1 I. Stamatelos, C. T. Dinh, W. Lehnert and M. Shviro, *ACS Appl Energy Mater*, 2022, **5**, 13928–13938.

2 W. Luo, J. Zhang, M. Li and A. Züttel, *ACS Catal*, 2019, **9**, 3783–3791.

3 J. Lee, J. Lim, C. W. Roh, H. S. Whang and H. Lee, *Journal of CO2 Utilization*, 2019, **31**, 244–250.

4 W. Luo, Q. Zhang, J. Zhang, E. Moioli, K. Zhao and A. Züttel, *Appl Catal B*, DOI:10.1016/j.apcatb.2020.119060.

5 J. Zeng, M. Fontana, A. Sacco, D. Sassone and C. F. Pirri, *Catal Today*, 2022, **397–399**, 463–474.

6 S. Zhu, X. Ren, X. Li, X. Niu, M. Wang, S. Xu, Z. Wang, Y. Han and Q. Wang, *Catalysts*, DOI:10.3390/catal11050535.

7 Y. Song, Y. Wang, J. Shao, K. Ye, Q. Wang and G. Wang, *supporting information Boosting CO 2 Electroreduction via The Construction of A Stable ZnS/ZnO Interface*.